Preprints of the 21st IFAC World Congress (Virtual)
Berlin, Germany, July 12-17, 2020

Error Analysis of ADRC Linear Extended State Observer for the System with Measurement Noise

Jia Song*. Mingfei Zhao*. Ke Gao*. Jiangcheng Su*.

* *School of Astronautics, Beihang University, Beijing, 100191, China (e-mail: songjia@buaa.edu.cn)*

Abstract: The Active Disturbance Rejection Control (ADRC) method, which is not dependent upon the accurate system model and has strong robustness for adjusting to disturbances, is widely used in many fields. As the core of the ADRC method, the performance of the Extended State Observer (ESO) is of great importance to the controller. In practical applications, the observer will inevitably receive the influence of measurement noise, but the research on the extent of impact is less. This article takes into account observing errors caused by measurement noise, deriving and analyzing their impact on Linear Extended State Observer (LESO) performance firstly. According to the theoretical derivation and simulation analysis, an improved controller is designed, which can effectively suppress the effect of noise on the actuator and system output.

Keywords: Linear Extended State Observer (LESO), Active Disturbance Rejection Control (ADRC), Measurement noise, Error analysis.

1. INTRODUCTION

In recent years, the theoretical research and engineering application of the Active Disturbance Rejection Control (ADRC) have been developed rapidly. Compared with modern control theory, ADRC inherits the advantages of non-system-based model of PID control (Han, J.Q., 2002). The ADRC is now considered to be an effective control strategy in solving the problems with uncertainty and time-delay (Guo, B.Z., Wu, Z.H., & Zhou, H.C., 2016; Wang, L., Li, Q., & Tong, C., 2013). The control structure of ADRC is very general, so it is widely used in many fields such as power system, precision instrument, aerospace, energy and chemical industry (Chang, K., Xia, Y., & Huang, K., 2016; Gao, K., Song, J., Wang, X., & Li, H.F., 2019; Huang, Y., & Xue, W., 2014; Jia, S., Ke, G., & Lun, W., 2016; Liu, F., Li, Y., & Cao, Y., 2016; Song, J., Gao, K., Wang, L., et al., 2016; Song, J., Lin, J., & Wang, L., 2017; Song, J., Wang, L., Cai, G., et al., 2015). However, it is difficult to tune the ADRC parameters perfectly, Gao therefore proposed a simplified control structure LADRC and the parameter tuning process (Gao, Z., 2003).

The Extended State Observer (ESO) is the basis of ADRC and it plays a role of estimating the total disturbance which includes unknown parts of the system and external disturbances. In addition, the ESO also works with sliding mode, projected gradient algorithm and other methods as an important component (Jiang, T., Huang, C., & Guo, L., 2015; Wang, L., Jian-Bo, S.U., & Automation, D.O., 2013; Xia, Y., Zhu, Z., & Fu, M., 2011). The Linear Extended State Observer (LESO) is constructed by linear functions, which is the constituent of LADRC and has the advantage of easy parameter tuning. The performance of the ESO directly determines the performance of the above control method. Hence some papers conducted in-depth analyses of it. The observing error of the second-order ESO was firstly analyzed and a principle of parameter setting was given to improve the accuracy of the observation (Han, J.Q., & Zhang, R., 1999). For several typical perturbations, the capability of ESO was further analyzed (Yang, X., & Huang, Y., 2009). The most commonly used parameter tuning method is the Bandwidth-Parameterization method (Gao, Z., 2003). On this basis, a method based on settling time was proposed (Chen, X., Li, D., & Gao, Z., 2011). Some practical methods of configuring LESO parameters in engineering applications were further analyzed (Chao, Z., Zhu, J.H., & Gao, Y.K., 2014; Dong, Y., Xiao-Jun, M.A., & Zeng, Q.H., 2013). The stability analysis of ESO has been demonstrated by a variety of methods such as Popov criterion (Erazo, C., Angulo, F., & Olivar, G., 2012) and Lyapunov method (Zheng, Q., Gaol, L.Q., & Gao, Z., 2008). More general results about the effect of the all disturbance on the observing error were derived through time domain and frequency domain analysis (Shao, X.L., & Wang, H.L., 2015; Wang, H.Q., & Huang, H., 2013).

The studies mentioned above have mainly focused on the structure and the parameter tuning of ESO. There are also some works on the study of system with noisy measurement. Due to the large gain characteristic of ESO, the noise can be amplified significantly. The impact of noise in high-gain observer was studied by (Vasiljevic L. K., Khalil H. K., 2008). The upper-bound of estimation error related to the cut-off frequency and the order of observer were given. However, the characteristics in frequency domain are not analysed. In order to solve this problem, filters are added to remove the high frequency noise (Huang, C., & Wang, J., 2013; Wang, Y., Yao, Y., & Ma, K., 2008). But these methods have the disadvantage that the amplitude and phase of the control system will be affected. The filtered signal will make a large observing error when used in the state observer. Taking the filtered signal as another extended state is an improvement of the previous methods (Lin, F., Sun, H., & Zheng, Q., 2005), but it has a poor effect on high order systems and the increasing order makes it difficult to tune parameters. Switching between gain values seems to be a practical method to significantly supress estimation error under measurement noise (Prasov, A. A., & Khalil, H. K., 2013; Cheng, Y., Chen, Z., Sun, M., et al., 2018), but the characteristics of high-gain observer in frequency domain is not analysed. Therefore, error analysis in frequency domain and improvement for LESO with consideration of the measurement noise become an urgent problem to be solved. For this purpose, the effect of measurement noise on observation error of LESO is deduced in frequency domain theoretically for the first time. And an improved controller is proposed, which can effectively reduce the oscillations of the actuator and output caused by the measurement noise.

The paper is structured as follows. Section 2 deduces the transfer function of the total disturbance and measurement noise to observing error of LESO, and the influence of the measurement noise on the observing error is analyzed from the frequency domain and time domain. In section 3, an improved controller is presented and verified by simulation. Finally, the conclusion is given in section 4.

2. The influence of the measurement noise on LESO

A brief review of ESO will be presented below. An nth order nonlinear system can be expressed as follows:

$$\begin{cases} \dot{x}_1 = x_2 \\ \dot{x}_2 = x_3 \\ \vdots \\ \dot{x}_n = f + bu \\ y = x_1 \end{cases} \tag{1}$$

x_i is the state of system; f is the total disturbances; $u(t)$ is the control signal and $y(t)$ is the system measurement output. Suppose the first-order derivative of f exists and is bounded. Define $x_{n+1}=f$. Then, (1) can be rewritten as (2).

$$\begin{cases} \dot{x}_1 = x_2 \\ \dot{x}_2 = x_3 \\ \vdots \\ \dot{x}_n = x_{n+1} + bu \\ \dot{x}_{n+1} = \dot{f} \\ y = x_1 \end{cases} \tag{2}$$

The LESO for system (2) is (3).

$$\begin{cases} \varepsilon = z_1 - y \\ \dot{z}_1 = z_2 - \beta_1 \varepsilon \\ \dot{z}_2 = z_3 - \beta_2 \varepsilon \\ \vdots \\ \dot{z}_n = z_{n+1} - \beta_n \varepsilon + bu \\ \dot{z}_{n+1} = -\beta_{n+1} \varepsilon \end{cases} \tag{3}$$

where z_i, i=1, 2, … n+1 are the observations of states, β_i, i=1, 2, … n+1 are adjustable parameters which influences the performance of LESO.

Remark 1: Measurement noise is considered in this paper, denote that $y_0 = y + \delta = x_1 + \delta$, where y_0 represents the system outputs with measurement noise, and δ is the noise which is reasonable assumed as a white noise here.

Denote $e_i = z_i - x_i$, i=1, 2, … n+1, representing the error of ith order observer.

$$\varepsilon = z_1 - y_o = z_1 - (y + \delta) = e_1 - \delta \tag{4}$$

Substituting (4) into (3), the observer estimation error of LESO is defined as

$$\begin{cases} \dot{e}_1 = e_2 - \beta_1 e_1 + \beta_1 \delta \\ \dot{e}_2 = e_3 - \beta_2 e_1 + \beta_2 \delta \\ \vdots \\ \dot{e}_n = e_{n+1} - \beta_n e_1 + \beta_n \delta \\ \dot{e}_{n+1} = -\beta_{n+1} e_1 + \beta_{n+1} \delta - \dot{f} \end{cases} \tag{5}$$

Let $e = [e_1, e_2, \ldots, e_{n+1}]^T$, and then (4) can be expressed as follows:

$$\begin{cases} \dot{e} = Ae + Bu \\ A = \begin{pmatrix} -\beta_1 & 1 & 0 & \cdots & 0 \\ -\beta_2 & 0 & \ddots & \ddots & \vdots \\ \vdots & \vdots & \ddots & \ddots & 0 \\ -\beta_n & 0 & \cdots & 0 & 1 \\ -\beta_{n+1} & 0 & \cdots & \cdots & 0 \end{pmatrix}, \\ B = \begin{pmatrix} \beta_1 & 0 \\ \beta_2 & 0 \\ \vdots & \vdots \\ \beta_n & 0 \\ \beta_{n+1} & -1 \end{pmatrix}, u = \begin{pmatrix} \delta \\ \dot{f} \end{pmatrix} \end{cases} \tag{6}$$

The above equation is converted into a transfer function form. The inputs are δ and $\dot{f}$. The output is e.

$$E(s) = \begin{Bmatrix} \dfrac{\sum_{k=1}^{n+1} \beta_k s^{n+i-k}}{|sI - A|} \\ \vdots \\ \dfrac{\sum_{k=i}^{n+1} \beta_k s^{n+i-k}}{|sI - A|} \\ \vdots \\ \dfrac{\beta_{n+1} s^n}{|sI - A|} \end{Bmatrix} \delta - \begin{Bmatrix} \dfrac{1}{|sI - A|} \\ \vdots \\ \dfrac{\sum_{k=0}^{k=i-1} \beta_k s^{i-k-1}}{|sI - A|} \\ \vdots \\ \dfrac{\sum_{k=0}^{k=i-1} \beta_k s^{i-k-1}}{|sI - A|} \end{Bmatrix} \dot{f}(\cdot) \tag{7}$$

The Bandwidth-Parameterization method (Gao, Z., 2003) is introduced for further analysis without loss of generality.

$$\begin{aligned} |sI-A| &= \beta_0 s^{n+1}+\beta_1 s^n+\cdots+\beta_n s+\beta_{n+1} \\ &= (s+\omega_0)^{n+1} \end{aligned} \tag{8}$$

where $\beta_i = C_{n+1}^i \omega_0^i$, ω_0 denotes the bandwidth, which is the only parameter to tune. Substituting (8) into (7), the transfer function is deduced ultimately. In this paper, we take third-order LESO as an example. The error transfer function of third-order LESO is expressed as follows:

$$\begin{aligned} E_1(s) &= \frac{s}{(\frac{s}{\omega_0}+1)^3}\dot{f}+\frac{\frac{3}{\omega_0^2}s^2+\frac{3}{\omega_0}s+1}{(\frac{s}{\omega_0}+1)^3}\delta \\ E_2(s) &= \frac{\frac{3}{\omega_0^2}\left(\frac{s/\omega_0}{3}+1\right)s}{(\frac{s}{\omega_0}+1)^3}\dot{f}+\frac{\left(\frac{s/\omega_0}{3}+1\right)s}{(\frac{s}{\omega_0}+1)^3}\delta \\ E_3(s) &= \frac{\frac{3}{\omega_0}\left(\frac{s^2/\omega_0^2}{3}+\frac{s}{\omega_0}+1\right)s}{(\frac{s}{\omega_0}+1)^3}\dot{f}+\frac{s^2}{(\frac{s}{\omega_0}+1)^3}\delta \end{aligned} \tag{9}$$

The effect of disturbance f has been analyzed in many papers, but the part of measurement noise δ has not been deduced. Here we analyze the latter separately.

$$\begin{aligned} E_1(s) &= \frac{\frac{3}{\omega_0^2}s^2+\frac{3}{\omega_0}s+1}{(\frac{s}{\omega_0}+1)^3}\delta \\ E_2(s) &= \frac{\left(\frac{s/\omega_0}{3}+1\right)s}{(\frac{s}{\omega_0}+1)^3}\delta \\ E_3(s) &= \frac{s^2}{(\frac{s}{\omega_0}+1)^3}\delta \end{aligned} \tag{10}$$

There is only one parameter ω_0 determines the character of the transfer function. ω_0 is usually selected as 3 to 5 times the desired closed loop natural frequency ω_c, which is selected according to the required time domain characteristics. We can set ω_0 to be 60 rad/sec and 100 rad/sec to explore the features of transfer function (10). First, we analyze the frequency domain characteristics according to the Bode plot.

The observing errors of the third-order ESO are shown in Fig.1. From left to right are the observing errors of the first, second and third order states respectively. From Fig.1, we can see that with the increase of ω_0, the frequency characteristic is shifted right. ω_0 also has a positive correlation with the gain in the middle frequency range.

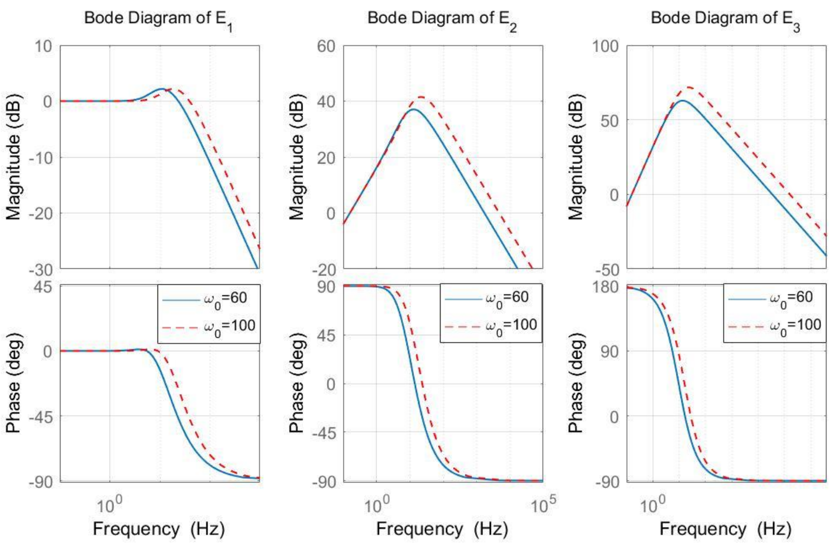

Fig. 1. Frequency responses of error transfer function

E_1 can be seen as a low-pass filter, which means that the low-frequency noise will make the observer produce the same error and high-frequency noise is suppressed. E_2 and E_3 can filter the low frequency and high frequency noise but have a large gain in the middle frequency range. For example, the magnitude curve of E_3 has a peak value of 71.7 dB when $\omega_0 = 100$ rad/sec. In this case, the observer will have an error of nearly 4000 times the measurement noise. Comparing the frequency responses of error transfer function with ω_0=60 and ω_0=100, the low frequency responses are similar. And with the increase of ω_0, the amplitude of high frequency signal is raising. The rate of magnifications of high frequency signal with different ω_0 is fixed with different frequency and related to the value of ω_0. More clearly results can be seen in the time domain map as shown in Fig. 2, where ω_0 is set as 100 rad/sec. A chirp signal with a frequency of 0.1 Hz to 300 Hz is chosen to test the error transfer functions. The noise signal is magnified 110 times by E_2, while 4000 times by E_3. Since the noise is distributed at full frequency, we can get the conclusion that observer of the higher rank state has the poorer performance, when measurement noise is comparatively large.

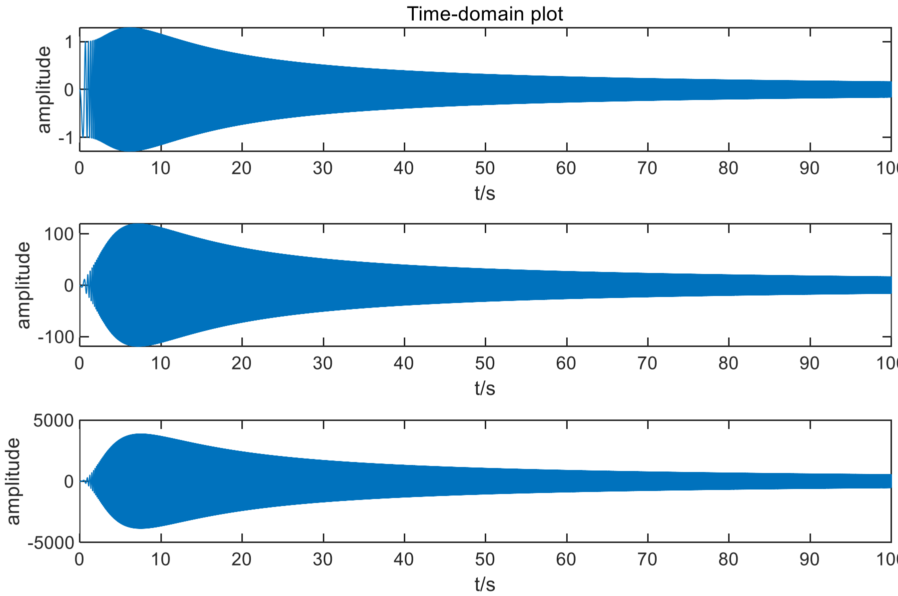

Fig. 2. Noise amplification effect in time domain

3. An improved controller design

Problem statement: The accuracy of LESO is affected when measurement noise is comparatively large. A novel controller design method is proposed to suppress the impact of measurement noise on system performance.

Consider a motion control test bed (Gao, Z., 2003) as the research object. Its mathematical model is a second-order dynamic system.

$$\ddot{y} = (a\dot{y} + b_0 T_d) + b_0 u \tag{11}$$

where u is control voltage, $T_d = -1$ is torque disturbance introduced at t=8s. $a = -1.41$, $b_0 = 23.2$ are unknown system parameters when we design the controller. b is the estimation of b_0 which is used in LESO.

Choose states $x_1 = y$ and $x_2 = \dot{y}$, according to system (1), the dynamic system (11) can be rewritten as

$$\begin{cases} \dot{x}_1 = x_2 \\ \dot{x}_2 = x_3 + b_0 u \\ x_3 = f = a\dot{y} + bT_d + (b - b_0)u \\ y = x_1 + T_n \end{cases} \tag{12}$$

The measurement noise T_n is 1% system output peak value white noise. And the total disturbance f is $a\dot{y} + bT_d + (b - b_0)u$. Then LESO is designed as system (3) with ω_0=60 and z_3 is the observation of x_3. The control law is designed as follows

$$\begin{aligned} & u = \frac{u_0 - z_3}{b_0},\ u_0 = k_p(r - z_1) - k_d z_2 \\ & k_d = 2\xi\omega_c,\ \omega_c = 10,\ \xi = 1,\ r = 1\ and\ k_p = \omega_c^2 \end{aligned} \tag{13}$$

Substituting (13) into (12),

$$\begin{cases} \dot{x}_1 = x_2 \\ \dot{x}_2 = x_3 - z_3 + u_0 \\ y = x_1 + T_n \end{cases} \tag{14}$$

The total disturbance x_3 is compensated in ADRC controller.

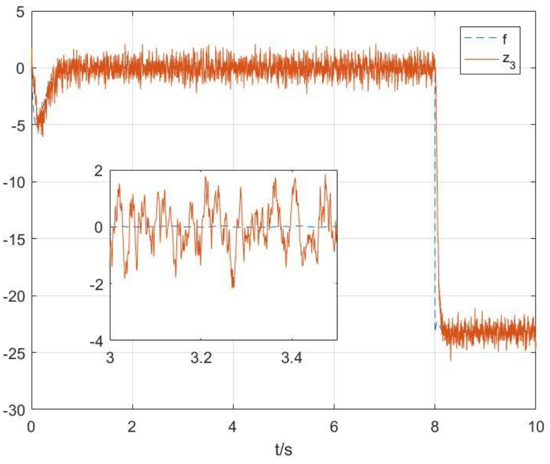

Fig. 3. Contrast of f and z_3

As shown in the Fig. 3, the blue line represents *f*, and the red line represents z_3. Before T_d is introduced, *f* is close to 0, while z_3 contains relatively large noise. The actuator violently shocks caused by useless noise and the system output will follow the shock. In this case, when z_3 is used as a part of the control signal, a poor control effect is obtained.

Remark 2: When $\text{abs}(b - b_0)$ is large, the signal-to-noise ratio of the feedback signal will be great due to the increase of *f*, but the observing error will increase. This phenomenon is very clear in the Fig. 4.

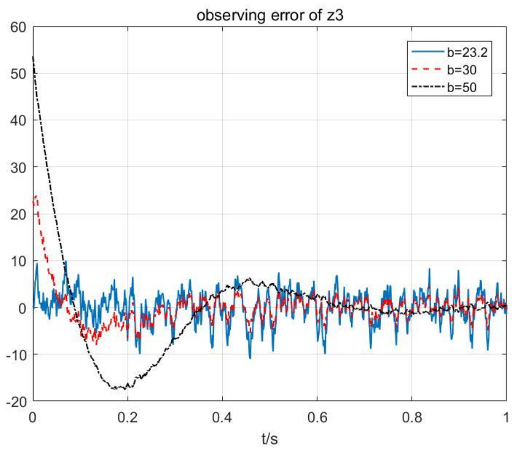

Fig. 4. Observing error of z_3

In order to reduce the oscillations of the actuator and system output caused by the measurement noise, we made the following improvements for the controller.

Definition: A noise filter threshold a_z is defined, which is based on the system's noise model and the observer parameters ω_0. Less than the threshold, z_3 will be adjusted when used in controller.

$$\begin{cases} \varepsilon = z_1 - y_o \\ \dot{x}_1 = x_2 \\ \dot{x}_2 = x_3 + bu \\ x_3 = f \\ \dot{z}_1 = z_2 - \beta_1 \varepsilon \\ \dot{z}_2 = z_3 - \beta_2 \varepsilon + bu \\ \dot{z}_3 = -\beta_3 \varepsilon \\ u = \dfrac{u_0 - fal(z_3, \alpha, \delta)}{b} \\ y = x_1 + T_n \end{cases} \tag{15}$$

where *fal* function is defined as (16), *α* is a number greater than 1 to reduce the gain due to large disturbances.

$$fal(\mathrm{e}, \alpha) = \begin{cases} \delta \left(\dfrac{|e| \tan(\dfrac{e}{4\delta}\pi)}{\delta} \right)^{\alpha} sign(e) & |e| < \delta \\ e & |e| \geq \delta \end{cases} \tag{16}$$

With the improved controller, the simulation results were got as follows. The parameters ω_0 and ω_c are 60 rad/sec and 10 rad/sec.

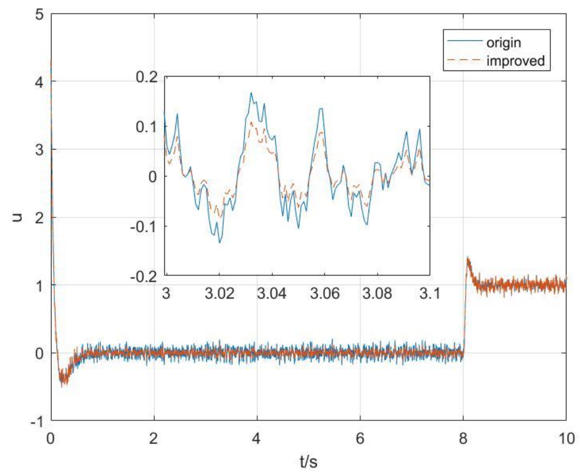

Fig. 5. Actuator instructions

Fig. 5 and Fig. 6 show the actuator output and system output respectively. The blue line represents the results of original controller, and the red line is the improved one. It can be seen from the simulation results that without affecting the other characteristics of the system, the improved controller can effectively reduce the output of the actuator and the fluctuations amplitude of system output caused by the measurement noise.

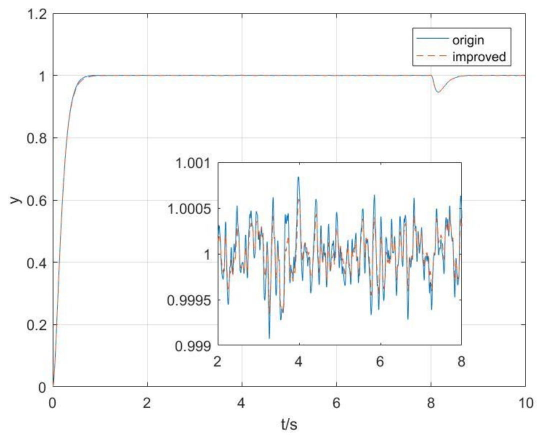

Fig. 6. System output

4. CONCLUSIONS

Measurement noise inevitably exists in actual system, which leads to the observing error. This paper analyzes the impact of measurement noise on LESO theoretically. On this basis, an improved controller is proposed. When the measurement noise is relatively large, the total disturbance will be seriously polluted by the high-gain amplified noise. The impact of measurement noise is suppressed by reducing the feedback gain using the *fal* function. The simulation results show that the improved controller can restrain the oscillation caused by the measurement noise. Therefore, the theoretical analysis and improvement of the controller have practical value in actual system.

5. FUNDING

This work was supported by the National Natural Science Foundation of China (61473015, 91646108). The authors thank the colleagues for their constructive suggestions and research assistance throughout this study. The authors also appreciate the associate editor and the reviewers for their valuable comments and suggestions.

6. REFERENCES

Chang, K., Xia, Y., & Huang, K. (2016). Obstacle avoidance and active disturbance rejection control for a quadrotor. *Journal of Neurocomputing*, 190, 60-69.

Chao, Z., Zhu, J.H., & Gao, Y.K. (2014). Order and parameter selections for active disturbance rejection controller. *Control Theory & Applications*.

Chen, X., Li, D., & Gao, Z. (2011). Tuning method for second-order active disturbance rejection control. *Proceedings of Chinese control conference*, (pp. 6322-6327).

Dong, Y., Xiao-Jun, M.A., & Zeng, Q.H. (2013). Research on frequency-band characteristics and parameters configuration of linear active disturbance rejection control for second-order systems. *Control Theory & Applications*, 30(12), 1630-1640.

Erazo, C., Angulo, F., & Olivar, G. (2012). Stability analysis of the extended state observers by Popov criterion. *Theoretical and Applied Mechanics Letters*, 2(4), 40-43.

Gao, K., Song, J., Wang, X., & Li, H.F. (2019). Fractional-order PID linear active disturbance rejection control design and parameter optimization for hypersonic vehicles with the actuator faults. *Tsinghua Science and Technology*. DOI: 10.26599/TST.2019.9010041.

Gao, Z. (2003). Scaling and bandwidth-parameterization based controller tuning. *American Control Conference*, 2003. Proceedings of the. IEEE, (pp. 4989-4996).

Guo, B.Z., Wu, Z.H., & Zhou, H.C. (2016). Active Disturbance Rejection Control Approach to Output-Feedback Stabilization of a Class of Uncertain Nonlinear Systems Subject to Stochastic Disturbance. *IEEE Transactions on Automatic Control*, 61(6), 1613-1618.

Han, J.Q. (2002). From PID Technique to Active Disturbances Rejection Control Technique, *Control Engineering of China*, 9(3), 13-18.

Han, J.Q., & Zhang, R. (1999). Error analysis of the second order eso. *Journal of Systemsence & Mathematicalences*, 19(4), 465-471.

Huang, C., & Wang, J. (2013). Analysis of ADRC in the Present of Measurement Noise. *Electronics Optics & Control*, 20(7).

Huang, Y., & Xue, W. (2014). Active disturbance rejection control: methodology and theoretical analysis. *Isa Transactions*, 53(4), 963-976.

Jiang, T., Huang, C., & Guo, L. (2015). Control of uncertain nonlinear systems based on observers and estimators. *Automatica*, 59, 35-47.

Jia, S., Ke, G., & Lun, W. (2016). Comparison of linear and nonlinear active disturbance rejection control method for hypersonic vehicle. *Control Conference. IEEE*, (pp. 10759-10764.)

Liu, F., Li, Y., & Cao, Y. (2016). A two-layer active disturbance rejection controller design for load frequency control of interconnected power system. *IEEE Transactions on Power Systems*, 31(4), 3320-3321.

Lin, F., Sun, H., & Zheng, Q. (2005). Novel extended state observer for uncertain system with measurement noise. *Control Theory & Applications*, 22(6).

Shao, X.L., & Wang, H.L. (2015). Performance analysis on linear extended state observer and its extension case with higher extended order. *Control & Decision*.

Song, J., Gao, K., Wang, L., et al. (2016). Comparison of linear and nonlinear active disturbance rejection control method for hypersonic vehicle. *The 35th Chinese Control Conference (CCC). IEEE*.

Song, J., Lin, J., & Wang, L. (2017). Nonlinear FOPID and Active Disturbance Rejection Hypersonic Vehicle Control Based on DEM Biogeography-Based Optimization. *Journal of Aerospace Engineering*, 30(6).

Song, J., Wang, L., Cai, G., et al. (2015). Nonlinear fractional order proportion-integral-derivative active disturbance rejection control method design for hypersonic vehicle attitude control. *Acta Astronautica*, 111, 160-169.

Wang, H.Q., & Huang, H. (2013). Property and applications of extended state observer. *Control & Decision*, 28(7), 1078-1082.

Wang, L., Jian-Bo, S.U., & Automation, D.O. (2013). Attitude tracking of aircraft based on disturbance rejection control. *Control Theory & Applications*, 30(12), 1609-1616.

Wang, L., Li, Q., & Tong, C. (2013). Overview of active disturbance rejection control for systems with time-delay. *Control Theory & Applications*, 30(12), 1521-1533.

Wang, Y., Yao, Y., & Ma, K. (2008). A new type extended state observer for system with measurement noise. *IEEE International Conference on Automation and Logistics*, (pp. 1745-1749).

Xia, Y., Zhu, Z., & Fu, M. (2011). Back-stepping sliding mode control for missile systems based on an extended state observer. *IET control theory & applications*, 5(1), 93-102.

Yang, X., & Huang, Y. (2009). Capabilities of extended state observer for estimating uncertainties. *Conference on American Control Conference. IEEE Press*, (pp. 3700-3705).

Zheng, Q., Gaol, L.Q., & Gao, Z. (2008). On stability analysis of active disturbance rejection control for nonlinear time-varying plants with unknown dynamics. *Decision and Control, 2007, IEEE Conference on. IEEE*, (pp. 3501-3506).

Vasiljevic, L. K., & Khalil, H. K. (2008). Error bounds in differentiation of noisy signals by high-gain observers. *Systems & Control Letters*, 57(10), 856-862.

Cheng, Y., Chen, Z., Sun, M., et al. (2018). Cascade Active Disturbance Rejection Control of a High-Purity Distillation Column with Measurement Noise. *Industrial & Engineering Chemistry Research*, 57(13).

Prasov, A. A., & Khalil, H. K. (2013). A Nonlinear High-Gain Observer for Systems With Measurement Noise in a Feedback Control Framework. *IEEE Transactions on Automatic Control*, 58(3), 569-580.